IIETA International Information and Engineering Technology Association
Advancing the World of Information and Engineering

Annales de Chimie - Science des Matériaux
Vol. 50, No. 3, June, 2026, pp. 227-240
Journal homepage: http://iieta.org/journals/acsm

Sustainable Use of Recycled Ceramic Waste for the Stabilization of Collapsible Soils in Semi-Arid Regions

Boussahel Hamza*, Bakir Nassima, Tallah Naoui

L.M.M.S. Laboratory, Faculty of Technology, Department of Civil Engineering, University M'sila, M'sila 28000, Algeria

Corresponding Author Email: hamza.boussahel@univ-msila.dz

https://doi.org/10.18280/acsm.500303

Received: 9 March 2026
Revised: 11 April 2026
Accepted: 19 April 2026
Available online: 30 June 2026

Keywords:
collapsible soils, recycled ceramic waste, sustainable stabilization, semi-arid regions, microstructural analysis, geotechnical performance

ABSTRACT

The sustainable management of industrial waste has become a key challenge in modern geotechnical engineering. This study examines the sustainable use of finely ground recycled ceramic waste (CW) as an alternative stabilizer for collapsible soils commonly found in semi-arid regions. Reconstituted specimens prepared from 80% Boussaâda sand and 20% Djebel Debbagh kaolin were treated with 4–8% CW and evaluated through Atterberg limits, Standard Proctor compaction, oedometer collapse, and unconsolidated–undrained triaxial shear tests. Microstructural analyses were performed using scanning electron microscopy (SEM) and energy-dispersive X-ray (EDX) spectroscopy. The inclusion of CW significantly reduced the plasticity index (from 8.66% to 4.24%), increased maximum dry density to 1.96 g/cm³, and lowered collapse potential from 11.7% to below 1% under high compaction energy. Cohesion improved substantially from 16 kPa to 105 kPa, while the internal friction angle decreased moderately from 35.46° to 29.93°, attributable to the replacement of coarse granular contacts by finer ceramic particles that reduce intergranular interlocking. SEM/EDX results revealed denser particle structures and the formation of calcium silicate hydrate (C–S–H) and calcium-aluminosilicate hydrate (C–A–S–H) gels. These findings confirm that recycled CW represents a sustainable, eco-efficient, and cost-effective solution for improving the performance of collapsible soils in semi-arid environments.

1. INTRODUCTION

Some soil types—particularly loess—exhibit an open, metastable structure characterized by high void ratios and apparent strength when dry or partially saturated. However, upon wetting, this fragile structure may rapidly collapse due to the loss of matric suction and the weakening of interparticle bonds, leading to a sudden and significant volume reduction commonly referred to as hydrocollapse. This abrupt settlement can result in serious structural failures, potentially affecting foundations, roadways, pipelines, and other subsurface infrastructure.

Loess deposits are among the most widespread collapsible soils globally, with extensive distribution across the Chinese Loess Plateau, Central Asia, Eastern and Central Europe, and the Great Plains of North America [1-4]. In North Africa, collapsible soil layers have been reported in Algeria, Egypt, and Morocco—particularly in semi-arid regions such as the Hauts Plateaux, the Aurès Mountains, and the steppe zones, where annual evaporation significantly exceeds precipitation [5-7].

From a geotechnical perspective, collapsible soils are typically marked by low dry density, medium to low plasticity, high macro-porosity, and a honeycomb-like skeletal structure held together by clay or carbonate bridges [8-10]. These soils often appear stable in their dry, natural state, yet can experience collapse strains ranging from 10% to 20% upon saturation [11, 12]. Standard laboratory procedures used to assess collapse potential include the double oedometer and single oedometer collapse index tests [13, 14], often supplemented by in-situ methods such as the Cone Penetration Test/Cone Penetration Test with Pore Pressure measurement (CPT/CPTu) and the standard penetration test (SPT), which provide valuable information on stratigraphy and soil strength [15, 16]. More advanced techniques—such as suction-controlled oedometer or triaxial testing, as well as scanning electron microscopy (SEM)—have significantly enhanced our understanding of the microstructural and hydro-mechanical mechanisms responsible for collapse behavior [17-19].

Mitigation strategies for collapsible soils generally fall into three categories: densification, drainage control, and chemical or mineralogical stabilization. Conventional methods include dynamic compaction [20, 21], soil replacement, and pre-wetting under surcharge loading. Chemical stabilization using lime, cement, or fly ash remains widely practiced, although concerns related to environmental impact, energy consumption, and cost persist [22-24]. In the North African context, localized treatments such as potassium chloride solutions or fiber reinforcements have shown promise, improving collapse resistance by altering the soil's microstructure and reducing porosity [25, 26]. In recent years, growing interest in sustainable and eco-efficient alternatives has led to the exploration of novel materials such as biopolymers (e.g., gelatin, alginate, xanthan gum) [27, 28], shredded rubber, and geopolymer systems derived from calcium carbide residue and sulfonic acid activators [29].

Within this broader trend, ceramic waste (CW)—a by-product of the ceramic and construction industries—has emerged as a promising stabilizer. Due to its composition rich in silica, alumina, and calcium oxide, CW exhibits pozzolanic properties that enhance interparticle bonding and reduce the soil's susceptibility to collapse. Prior research has demonstrated that CW can improve the strength and durability of cementitious materials [30-33]. In geotechnical applications, CW powder (CWP) has been shown to increase dry density, reduce plasticity, and enhance cohesion in soils [34-36]. It has been reported that waste ceramic dust reduces plasticity and improves compaction and strength characteristics [37], while significant improvements in dry density, unconfined compressive strength (UCS), and California bearing ratio (CBR) values have been observed in soils treated with CW [34, 36]. Similarly, the combined use of waste ceramic dust and lime has been shown to substantially improve the geotechnical behavior of expansive soils subjected to prolonged leaching [38].

Nevertheless, despite these promising findings, the specific use of CW for stabilizing collapsible soils in arid and semi-arid regions remains underexplored—particularly in North African environments, where such solutions could have both technical and environmental advantages. This work fills this gap by experimentally investigating the use of finely ground CW (4–8%) to stabilize reconstituted collapsible soil composed of Boussaâda sand (80%) and Djebel Debbagh kaolin (20%), utilizing locally sourced Algerian materials. Alterations in index properties (Atterberg limits), compaction characteristics (Standard Proctor), collapse potential (oedometer), and shear strength (unconsolidated–undrained triaxial) are evaluated, and the underlying mechanisms are analyzed through SEM/EDX. The objectives are to: (i) assess the impact of CW dosage on plasticity, density, collapse potential, and unconsolidated undrained strength parameters; (ii) clarify the microstructural bonding and gel formation that support macroscale performance; and (iii) evaluate the viability of CW as an economical, circular stabilizer for infrastructure in arid and semi-arid regions of North Africa.

2. MATERIALS AND METHODS

2.1 Materials

This study employed locally sourced geomaterials and industrial by-products obtained from various regions of Algeria. The coarse fraction consisted of natural sand from the Boussaâda region, with particle sizes under 2 mm. The fine fraction was derived from kaolin, a clay-rich material extracted from Djebel Debbagh in Guelma, which was ground to particles smaller than 80 µm to ensure uniformity and improve its interaction with the sandy matrix. Additionally, CW collected from municipal solid waste sites in Aïn Azel (Sétif) was finely milled to below 80 µm and used as a supplementary component. These materials were combined to create a reconstituted soil composed of 80% sand and 20% kaolin. Based on established collapse criteria in the literature [7, 8, 11], this formulation is classified as collapsible soil. A detailed overview of the physical properties of both the sand and the fine-grained additives is presented in Table 1.

The chemical compositions of the different materials used in this study are summarized in Table 2.

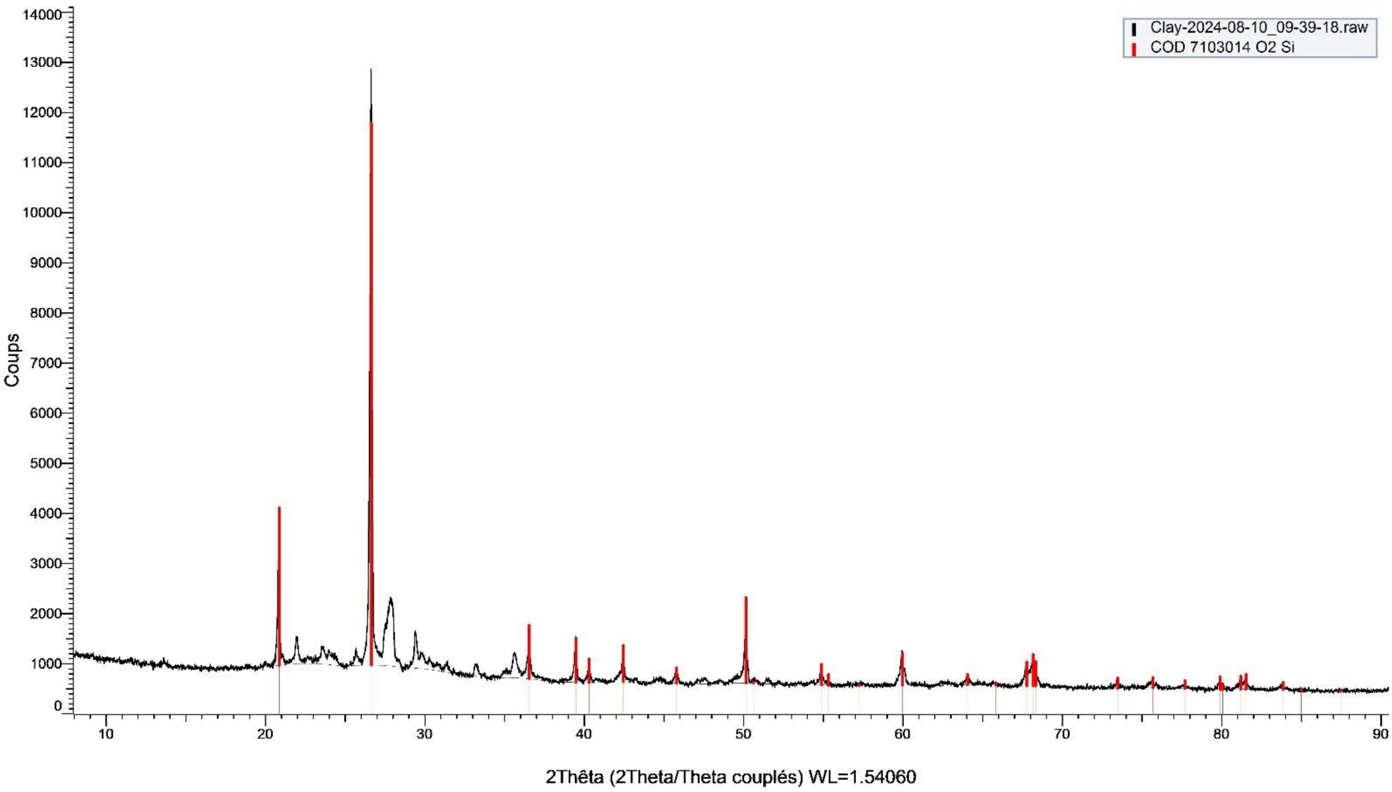

Figure 1. X-ray diffractogram of ceramic powder

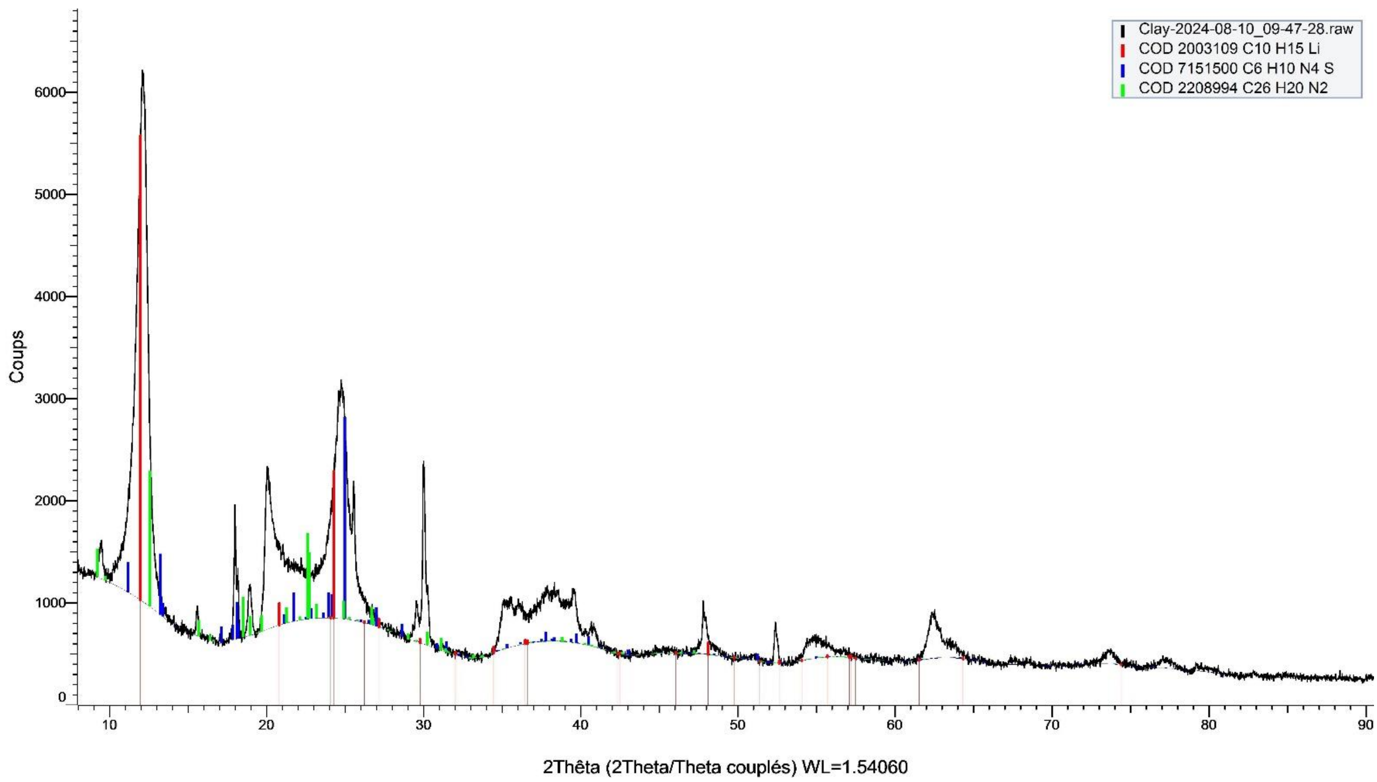

Figure 2. X-ray diffractogram of kaolin

Table 1. Geotechnical characteristics of the constituents and the reconstituted soil

Material	Sand	Kaolin	Reconstituted Soil
Sand equivalent E_s %	87.0	-	-
Coefficient of uniformity C_u	2.35	-	-
Coefficient of curvature C_c	1.08	-	-
Specific density γs (g/cm^3)	2.62	2.50	2.54
Liquid limit W_l%	-	56.10	24.96
Plastic limit W_p%	-	32.47	16.30
plasticity index Ip		23.63	8.66
Maximum dry density γ_d (g/cm^3)	-	-	1.91
Optimal water content w_{opt}%			10.57

To better understand the microstructure and mineral content of the materials, X-ray diffraction (XRD) analysis was performed. Considering the ceramic powder first (Figure 1), the XRD pattern highlights quartz—essentially silicon dioxide (SiO_2)—as the dominant crystalline phase. This is evident from a strong reflection around the 2θ angle of approximately 26.6°. Several secondary peaks further confirm the high quartz content, which is consistent with earlier findings on the pozzolanic behavior of ceramic powders [30-32, 35].

Table 2. Chemical compositions of the different materials used

Constituents (%)	Sand	Kaolin	Ceramic
SiO_2	93.38	40.68	63.61
Al_2O_3	0.90	37.57	14.56
Fe_2O_3	0.52	0.13	4.56
CaO %	2.06	0.41	8.41
MgO	0.20	0.19	1.57
SO_3 %	0.16	0.20	0.24
K_2O %	0.31	0.50	2.79
Na_2O	0.54	0.27	1.16

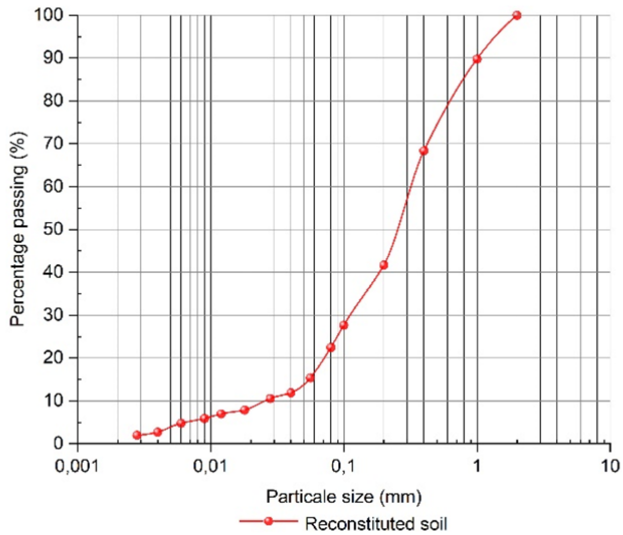

Figure 3. Grain size distribution curve of the reconstituted soil

The kaolin sample, on the other hand, revealed a more complex and mixed mineralogy in its diffractogram (Figure 2). Several distinct phases were detected: kaolinite, identified by a pronounced peak near 2θ ≈ 12°; muscovite around 2θ ≈ 20–21°; and microcline feldspar with peaks in the 27° to 30° range. Additionally, a scattering of smaller and broader peaks suggests the presence of amorphous material and possibly minor organic content. These observations are consistent with results reported in previous studies on kaolin-rich soils, which commonly indicate similarly complex mineral assemblages [4, 17, 18].

Table 1 provides a summary of the laboratory-reconstituted soil's geotechnical properties, and Figure 3 displays the particle size distribution curve.

2.2 Methods

In accordance with ASTM D4318 [39], the Atterberg limits were determined for soil samples mixed with varying proportions of CW. These tests served as an initial assessment of the plasticity characteristics of both the natural collapsible soil and the soil–CW blends. All key tests (Atterberg limits, Standard Proctor, oedometer, and unconsolidated–undrained (UU) triaxial) were performed in triplicate (n = 3). Results are reported as mean ± standard deviation (SD). Variability is shown as error bars in the corresponding figures.

Subsequent to this characterization, one-dimensional consolidation tests were conducted on dry samples, following ASTM D5333 [40]. For specimen preparation, a custom-designed laboratory compaction hammer was used (Figure 4). The collapse potential was evaluated through inundation under load, as outlined in ASTM D5333 [40]. Tests were carried out under different compaction energies (20, 40, and 60 blows) and initial moisture contents of 2%, 4%, and 6%. Both untreated and CW-amended soils were analyzed to assess the impact of ceramic additives on collapse behavior. The degree of collapse was classified based on the criteria presented in Table 3 [11].

Table 3. Collapse potential values

Cp (%)	Severity of Disorders
0-1%	No problem
1-5%	Moderate trouble
5-10%	Trouble
10-20%	Severe trouble
>20%	Very severe trouble

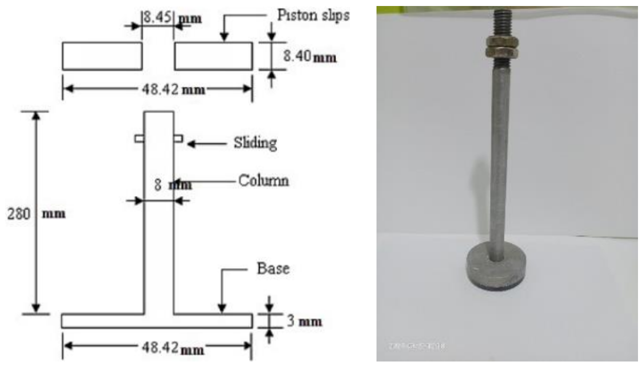

Figure 4. Compaction equipment

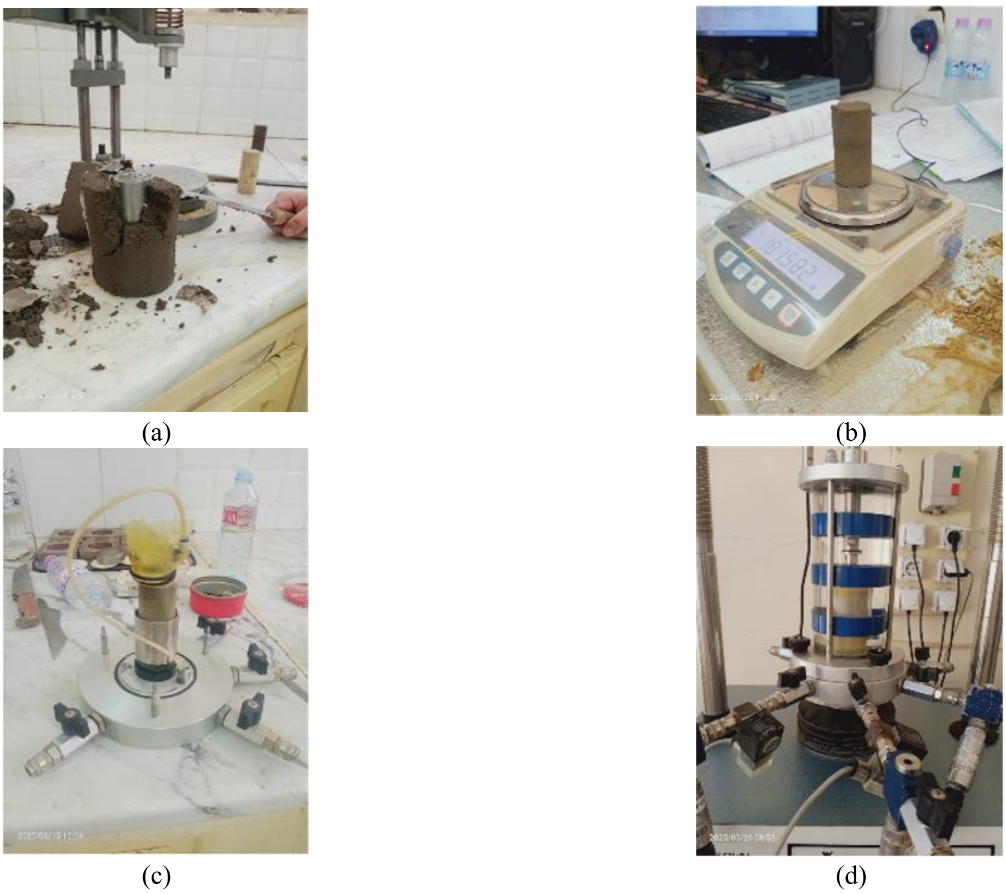

Figure 5. Specimen preparation and testing sequence for unconsolidated–undrained (UU) triaxial shear test: (a) extraction from the mold, (b) weighing of cylindrical specimen, (c) placement in the triaxial cell, and (d) final positioning of the specimen within the triaxial apparatus

Following identification of the optimal compaction parameters, Standard Proctor tests were performed in accordance with ASTM D698 [41] to determine the maximum dry density (γdmax) and optimum moisture content (wopt). CW was incorporated in quantities ranging from 4% to 8% by weight of the oven-dried natural soil. After quantifying collapse potential, the mechanical behavior of the samples was further investigated through unconsolidated–undrained (UU) triaxial tests, in accordance with ASTM D2850 [42]. Cylindrical specimens with dimensions of 36 mm in diameter and 76 mm in height were prepared under the same compaction conditions as those used in the Standard Proctor tests. The specimens were extracted from molds using a cutting ring (Figure 5). Triaxial tests were conducted under confining pressures of σ = 100, 200, and 300 kPa to determine shear strength parameters, namely cohesion (c) and internal friction angle (φ). The UU triaxial test was selected to represent the short-term, undrained loading condition, which is most relevant for rapid construction scenarios on unsaturated collapsible soils in arid and semi-arid climates. Under such conditions, excess pore pressures are not dissipated during loading, and the UU test provides a conservative estimate of the soil's immediate bearing capacity. The specimens were tested at their as-compacted moisture and density state, without prior consolidation, consistent with ASTM D2850 [42].

In parallel with the geotechnical tests, microstructural investigations were carried out using SEM combined with energy-dispersive X-ray spectroscopy (SEM/EDX) on both untreated (native) soil and soil–CW blends (4–8% CW). High-vacuum SEM images acquired in secondary-electron (SE) mode were used to evaluate grain morphology, particle contacts, and surface texture. EDX spectra were obtained to identify the principal elemental constituents of the matrix and additives (major elements: O, Si, Al, Ca; minor elements: Fe, K, Na, Mg, S; sporadic Mo). These SEM/EDX observations complement the geotechnical results by providing microstructural and chemical insight into the stabilization mechanisms achieved using CW alone.

3. RESULTS AND DISCUSSIONS

3.1 Atterberg limits

Plasticity index method is used for estimating the CW content (as a stabilizer) in soil. The results of Atterberg limit tests conducted on the samples with different contents of CW are presented in Table 4 and Figure 6. According to the experimental findings, the addition of CW to collapsible soil resulted in a slight increase in the Plastic Limit from 16.30% to 18.36%, a decrease in the Liquid Limit from 24.96% to 22.6%, and a decrease in the Plasticity Index from 8.66% to 4.24%. These alterations are explained by the substitution of inert ceramic particles for active clay minerals, which lessen plasticity and water absorption. This alteration reduces moisture-induced collapse in collapsible soils, improving structural stability.

Table 4. Atterberg limits value versus ceramic waste (CW) content

Ceramic Waste Content %	Liquid Limit (Mean ± SD)	Plastic Limit (Mean ± SD)	Plasticity Index (Mean ± SD)
0	24.96±0.78	16.30±0.51	8.66±0.29
4	24.46±0.64	17.23±0.48	7.23±0.30
6	23.62±0.76	17.54±0.66	6.08±0.19
8	22.60±0.89	18.36±0.77	4.24±0.12

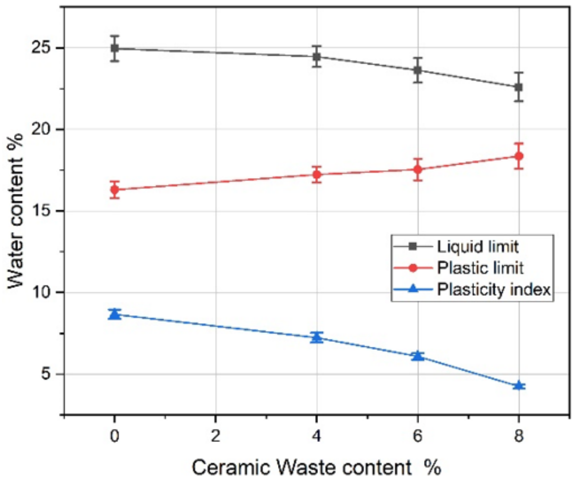

Figure 6. Variation of Atterberg limits with ceramic waste content (CW)

3.2 Standard compaction results

Figure 7 shows the results of the standard Proctor compaction tests, while Table 5 outlines how different amounts of CW (4%, 6%, and 8%) affect the soil's dry density and optimum moisture content (O.M.C.). At 4% CW, the dry density increases slightly to 1.93 g/cm³, which is a bit higher than the untreated soil, suggesting that the CW has a minimal effect on compaction. The O.M.C. drops just a little to 10.48%, down from 10.57% for the untreated soil, indicating that the CW has a mild influence on the soil's ability to retain moisture. When the CW is increased to 6%, the dry density reaches its highest value of 1.96 g/cm³, suggesting this amount of waste is the most effective for compaction. This is likely because the ceramic particles help the soil pack more efficiently. This also results in the lowest O.M.C. of 10.13%, showing that less water is needed for optimal compaction at this concentration. However, at 8% CW, the dry density decreases slightly to 1.89 g/cm³, and the compaction curve becomes flatter. The O.M.C. drops further to 9.98%, which shows that the higher amount of CW starts to disrupt the soil structure, creating voids that reduce the efficiency of compaction. Interestingly, the amount of water needed for optimal compaction decreases slightly as well.

These results align with studies by Chen and Idusuyi [43], who observed that the addition of CW improved compaction up to a certain threshold, beyond which further increases in CW caused a reduction in dry density. Similarly, Sabat and Pati [44] found that the addition of ceramic dust to expansive soils enhanced compaction, but beyond a certain limit, the effectiveness started to diminish. This study highlights the importance of finding an optimal level of CW for efficient soil compaction, reinforcing the notion that the interaction between CW and soil is crucial for optimizing compaction properties.

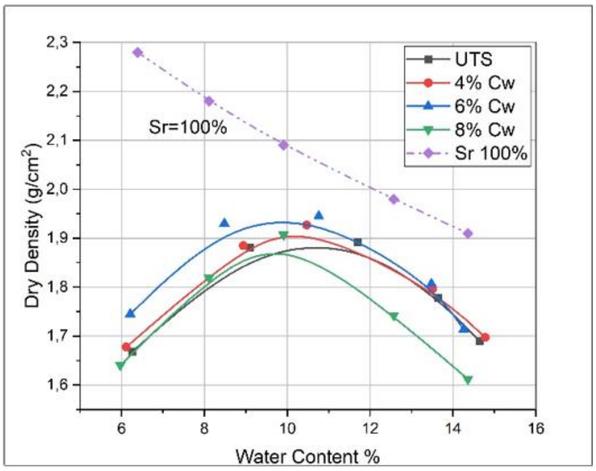

Figure 7. Effect of ceramic waste (CW) on optimum parameters of proctor test

Table 5. Optimum parameters of proctor test value versus ceramic waste (CW) content

Ceramic Waste Content %	O.M.C (%) (Mean ± SD)	M.D.D (g/cm^3) (Mean ± SD)
0	10.57±0.35	1.91±0.09
4	10.48±0.22	1.93±0.05
6	10.13±0.30	1.96±0.08
8	09.98±0.32	1.89±0.09

Note: M.D.D = Maximum Dry Density

3.3 Oedometer tests

3.3.1 Initial water content's effect on the collapse potential at various compaction energies

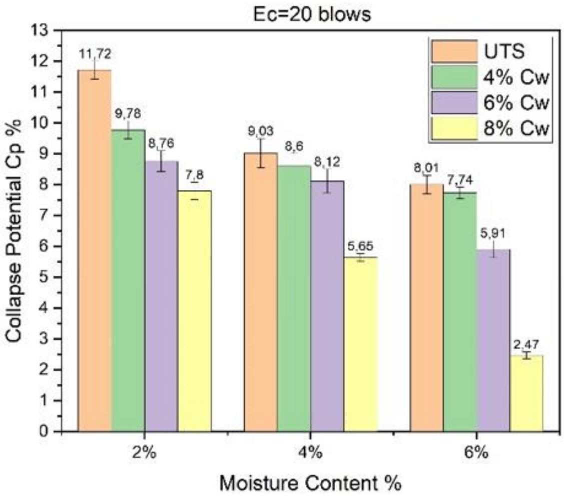

Figure 8. Variation of collapse potential (Cp) with initial water content under a compaction energy of 20 blows

Across all compaction energies of 20, 40, and 60 blows, respectively, and treatment levels of 4%, 6%, and 8% CW, the experimental results shown in Figures 8-10 demonstrate a consistent decrease in the collapse potential (Cp%) as the initial moisture content increases. Untreated soil showed a Cp of about 11.72% at 2% moisture under the lowest compaction energy (20 blows, Figure 8), indicating a high risk of collapse. On the other hand, Cp significantly decreased in soils treated with 8% CW, reaching about 7.80%. Cp values further decreased as compaction energy rose (Figures 9 and 10). The 8% CW-treated soil had a Cp below 1% at 60 blows and 6% moisture (Figure 10), which, in accordance with the Jennings and Knight [11] classification, corresponds to a non-collapsible soil.

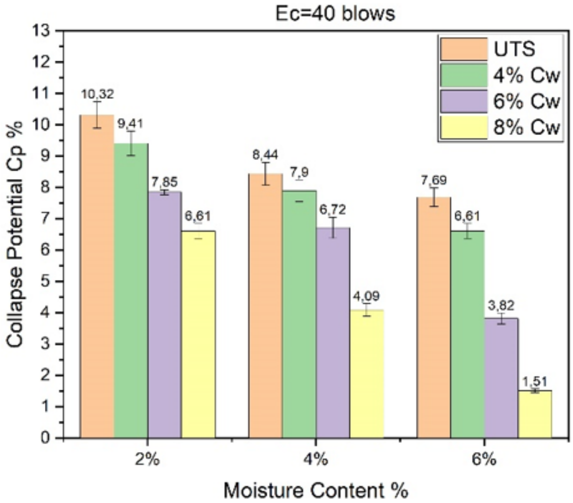

Figure 9. Variation of collapse potential (Cp) with initial water content under a compaction energy of 40 blows

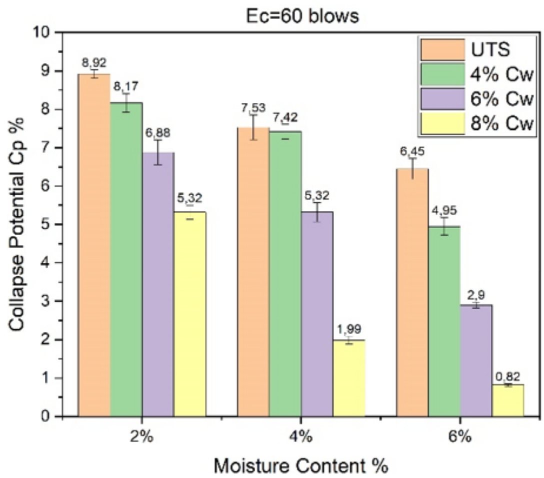

Figure 10. Variation of collapse potential (Cp) with initial water content under a compaction energy of 60 blows

3.3.2 Energy compaction's impact on the collapse potential

Figures 11-13 show how compaction energy affects the collapse potential (Cp) of soils with different moisture levels (4%, 6%, and 8%). The key takeaway is that as compaction energy increases, Cp goes down. Soils that were untreated had the highest Cp values, while soils with higher moisture content—especially at 8%—were more stable compared to those with 4% and 6% moisture.

There are a few reasons behind this. Compaction reduces the gaps between soil particles, allowing them to connect more tightly and lowering the chances of collapse. It also strengthens the bonds between particles, which boosts soil cohesion and stability. On top of that, compacted soil retains water better, which helps it stay more stable over time. Compaction also helps moisture spread evenly, making the soil more resilient to changes in the environment and less likely to fail. Lastly, compacting the soil puts more pressure on the fine particles, which helps them bond and distribute more evenly, especially in soils with higher moisture.

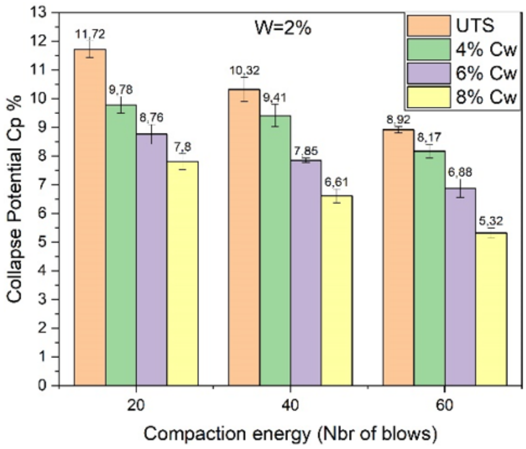

Figure 11. Effect of compaction energy on the collapse potential (Cp) (Moisture content W = 2%)

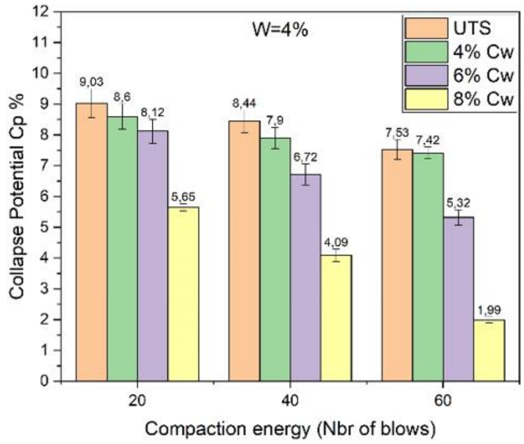

Figure 12. Effect of compaction energy on the collapse potential (Cp) (Moisture content W = 4%)

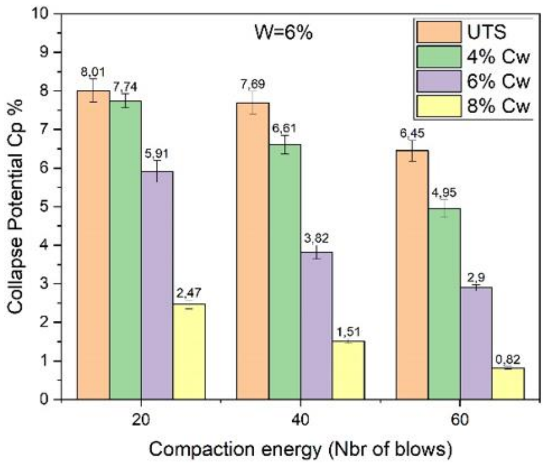

Figure 13. Effect of compaction energy on the collapse potential (Cp) (Moisture content W = 6%)

These results match what Bakir et al. [26] found in their study, where they showed that better compaction and higher moisture content can really reduce collapse potential and improve soil stability.

3.3.3 Influence of treatment content on the collapse potential

The experimental results show that adding CW significantly reduces the collapse potential (Cp) of treated soil, regardless of the moisture content (W = 2%, 4%, and 6%). As seen in Figure 14, at W = 2%, untreated soil has a Cp of 11.72% after 20 blows. However, when 8% CW is added, the Cp drops to 7.8%, a 33.6% improvement. In Figure 15, at W = 4%, the Cp decreases from 9.03% to 5.65% (a 37.7% improvement) with 8% CW, showing an even stronger stabilizing effect as moisture content increases. Figure 3 shows that at W = 6%, untreated soil starts with a Cp of 8.01%, but with 8% CW, it drops significantly to 2.47% (a 69.2% improvement). Additionally, when the compaction energy is increased to 40 blows, the Cp further decreases to 1.75% with 8% CW, indicating a substantial improvement. At 60 blows, as shown in Figure 16, the Cp reaches its lowest point at 0.82%, which is classified as "negligible collapse potential" and indicates a very low risk of collapse. This represents an additional reduction of about 53% compared to 40 blows.

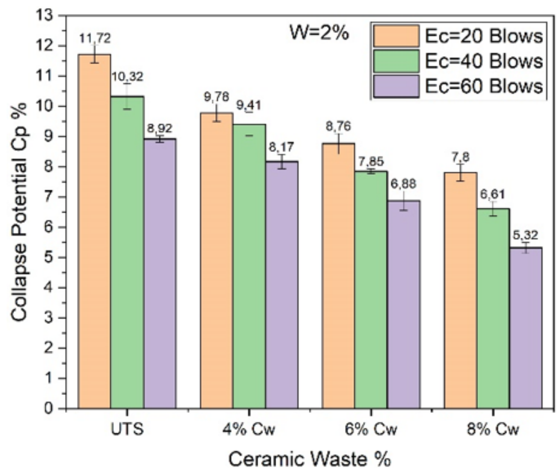

Figure 14. Influence of stabilizer content on collapse potential (Cp) at various compaction energy levels (Moisture content W = 2%)

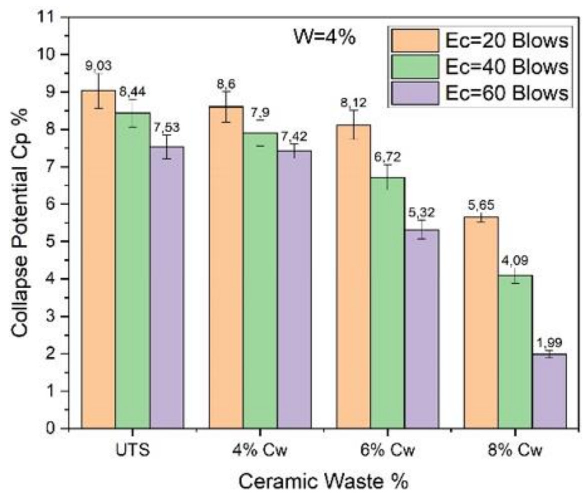

Figure 15. Influence of stabilizer content on collapse potential (Cp) at various compaction energy levels (Moisture content W = 4%)

Overall, these results emphasize the combined effect of CW, moisture content, and compaction. The greatest reduction in collapse potential occurs with higher compaction (Ec = 60 blows) and more CW. These findings confirm that CW, especially when paired with higher compaction and moisture levels, is an excellent stabilizer, greatly improving soil strength and minimizing the risk of collapse.

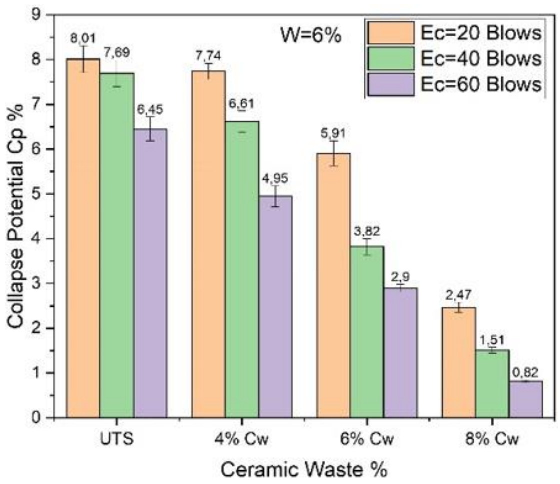

Figure 16. Influence of stabilizer content on collapse potential (Cp) at various compaction energy levels (Moisture content W = 6%)

3.4 Triaxial tests

3.4.1 Treatment's impact on the collapsible soil's behavior

The results of shear strength parameters of unconsolidated undrained (UU) tests on treated and non-treated soils are summarized in Table 6. When different amounts of CW were added to the soil, there was a noticeable shift in its shear strength properties—especially in terms of cohesion and internal friction angle. In its original, untreated state, the soil had very low cohesion—just 16 kPa—but a fairly high friction angle of 35.46°. This combination typically points to a soil that relies more on particle friction than on bonding to hold itself together.

However, once CW was introduced, things began to change quite significantly. Cohesion values started climbing steadily: at 4% CW, it reached 41 kPa; at 6%, it jumped to 65 kPa; and at 8%, it peaked at 105 kPa. What this suggests is that the CW helped particles stick together more effectively—possibly by filling in gaps between grains, promoting tighter packing, and even triggering some chemical bonding.

Interestingly, while cohesion was increasing, the friction angle went the other way. It dropped from 35.46° down to 29.93° as more CW was added. This drop likely comes from a change in the soil's internal structure. The finer ceramic particles may have disrupted the natural interlocking of soil grains, making the soil less dependent on friction and more on cohesion for its strength.

Table 6. Shear strength parameters of soil treated with different percentages of ceramic waste (CW)

Mix Type	Cohesion, c (kPa) (Mean ± SD)	Friction Angle, φ (°) (Mean ± SD)
Untreated soil	16±0.75	35.46±1.72
4% CW	41±1.05	33.98±1.33
6% CW	65±1.66	33.12±0.83
8% CW	105±4.65	29.93±1.46

Looking at the chemical makeup of the materials used (as shown in Table 2), it's easier to see why this is happening. The base sand was mostly silica—around 93.38%—which is basically inert and explains the soil's high friction angle but low cohesion before any treatment. Kaolin, on the other hand, has a high alumina content (about 37.57%) and brings more reactivity and plasticity into the mix. CW sits somewhere in the middle. It contains a good amount of silica (63.61%), some alumina (14.56%), and a notable portion of calcium oxide (around 8.41%).

These components, especially calcium oxide along with amorphous forms of silica and alumina, can trigger mild pozzolanic reactions under alkaline conditions. This can lead to the formation of bonding agents like calcium silicate hydrate (C–S–H) and calcium aluminate hydrate (C–A–H) gels, which help glue soil particles together. That would explain why cohesion improves with more CW, even though the friction angle drops a bit.

This behavior is consistent with the findings of other researchers. Lavat et al. [30] reported that ceramic roof tile waste exhibits pozzolanic activity, leading to the formation of secondary C–S–H phases. Matias et al. [33] further demonstrated that incorporating CW into lime mortars enhanced compressive strength. Similarly, Hoppe Filho et al. [32] observed microstructural changes in red ceramic waste–cement systems. In a review, Iravanian and Saber [35] emphasized that CW improves soil strength not only through physical reinforcement but also by promoting chemical interactions within the soil matrix.
Our findings corroborate previous studies indicating that ceramic by-products enhance interparticle bonding and reduce soil plasticity. Saber and Iravanian [37] reported improvements in compaction behavior and strength characteristics of clayey soils treated with ceramic dust, while Rathore and Tiwari [34] observed significant increases in dry density, UCS, and CBR values. Additionally, Blayi et al. [36] demonstrated that CW powder improves the geotechnical properties of clayey soils. Okeke [38] further demonstrated that the combination of ceramic dust with lime enhances the strength of expansive soils under prolonged leaching conditions. Extending this body of evidence, the present study confirms the effectiveness of CW in mitigating collapse potential and improving shear strength in collapsible soils subjected to arid environmental conditions.

According to Figure 17, Soils treated with varying amounts of CW—specifically 4%, 6%, and 8%—demonstrated a consistent trend: shear stress increased proportionally with confining pressure across all test samples. This aligns with the well-known behavior of soils becoming stronger under higher stress. In its untreated state, the soil showed the weakest shear resistance, with measured shear stresses of 162 kPa, 293.5 kPa, and 443.5 kPa under confining pressures of 100, 200, and 300 kPa, respectively. Once CW was introduced, however, there was a clear improvement in strength.

At just 4% CW content, the soil's shear stress rose to 200.3, 310.5, and 456.8 kPa. With 6% CW, the performance was even better—235, 360.7, and 478.9 kPa under the same pressure levels. The most notable gains came with the 8% mix, where shear strength peaked at 284.4, 379.4, and 486.2 kPa. These findings point to a key role played by CW in reinforcing the soil structure—primarily by enhancing interparticle bonds and reducing susceptibility to shear failure.

Interestingly, the impact of CW is most pronounced under low to moderate confining pressures, where treated samples show a stark difference compared to untreated ones. At higher confining pressures, the performance curves of all samples begin to converge. This suggests that while CW improves internal cohesion and structure, the effect of external pressure starts to overshadow these improvements at higher stress levels.

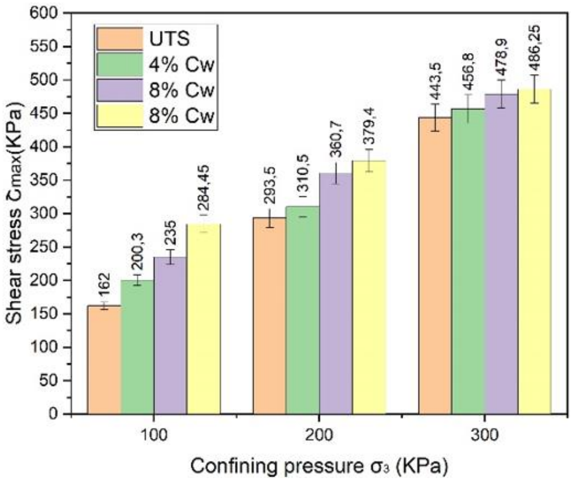

Figure 17. Effect of different ceramic waste (CW) contents on shear strength of soil under varying confining pressures

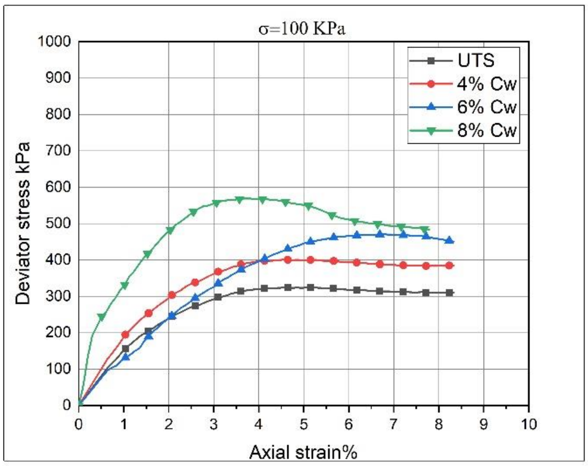

Figure 18. Effect of different ceramic waste (CW) contents on deviator stress-axial deformation behavior (σ = 100 KPa)

The stress–strain responses make it clear that upping the confining pressure from 100 to 300 kPa consistently boosts the peak deviator stress in both untreated and modified soil samples—an expected outcome tied to the classic confinement effect on shear strength. Adding ground CW shows a steady strengthening impact across the board. For instance, at 100 kPa (Figure 18), untreated soil hits around 324 kPa, while CW-treated versions reach about 400.6. kPa with 4% CW, 470 kPa at 6%, and roughly 568.9 kPa when 8% is added. The trend continues at 200 kPa (Figure 19), where strength rises from 587 kPa (untreated) to approximately 621, 721.4, and 758.8 kPa with increasing CW content. At 300 kPa (Figure 20), the figures climb further—going from 887 kPa up to around 913.6, 957.8, and 972.5 kPa as the CW percentage rises.

That said, the mixes with 8% CW tend to show a sharp strength drop after the peak, especially when the confinement is low. This suggests a brittle failure mode, likely due to the formation of a stiffer, more cemented structure that's vulnerable to localized cracking or collapse. On the other hand, the 6% CW mix not only delivers a notable strength boost but also maintains a smoother, more controlled decline after peak stress—pointing to better ductility and energy dissipation.

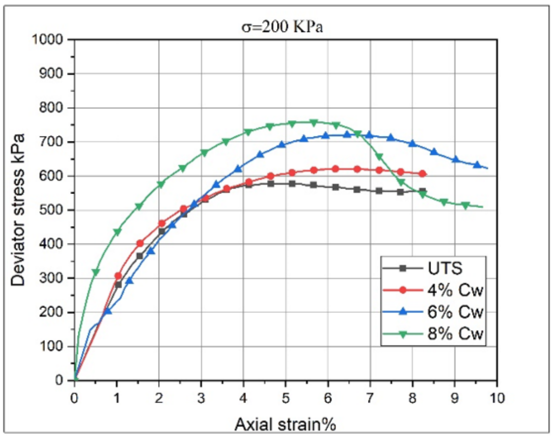

Figure 19. Effect of different ceramic waste (CW) contents on deviator stress-axial deformation behavior (σ = 200 KPa)

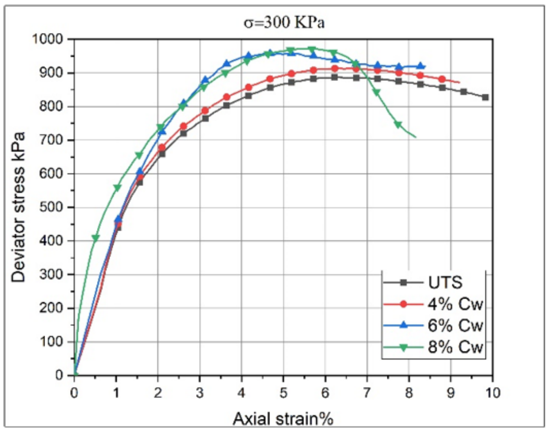

Figure 20. Effect of different ceramic waste (CW) contents on deviator stress-axial deformation behavior (σ = 300 KPa)

From a geotechnical standpoint, the main reason behind the strength gains appears to be an increase in apparent cohesion (c), likely driven by enhanced particle bonding, while the friction angle (φ) stays more or less stable. Stiffness at early loading stages also sees a noticeable bump with more CW in the mix. Taken together, the 6% dosage hits a sweet spot—offering a strong improvement in both peak strength and post-peak behavior across different confining pressures. Meanwhile, though 8% maximizes initial resistance, its brittleness could pose a risk in dynamic loading scenarios like earthquakes or repeated traffic loads. From an engineering standpoint, 6% CW is recommended as the balanced optimal dosage. At this content, maximum dry density (MDD) peaks (1.96 g/cm³), Cp is reduced below 5%, cohesion reaches 65 kPa, and failure mode remains ductile. 8% CW maximizes cohesion (105 kPa) and achieves Cp < 1% at 60 blows but induces brittle failure under low confinement and should be reserved for predominantly monotonic loading conditions (e.g., seismic events, traffic loads). Therefore, 8% CW should be considered only when maximum strength is required and loading conditions are predominantly monotonic and well-controlled.

3.5 Microstructural analysis with scanning electron microscopy and X-ray energy dispersive spectroscopy scanning

The SEM micrographs of the untreated sand–kaolin soil (Figure 21(a) and (b)) exhibit a heterogeneous, loosely arranged fabric characterized by significant interparticle gaps and minimal bonding, suggesting a rather porous structure. The EDX spectrum presented (Figure 21(c)) is predominantly characterized by O, Si, and Al, with modest contributions from Ca and tiny amounts of S, aligning with quartz-rich sand and kaolinitic phases. Conversely, the soil stabilized with 6% CW (Figure 22(a) and (b)) demonstrates a significantly denser and more cohesive texture: grains are interconnected by fine reaction products, and pore spaces are partially occluded, indicating improved particle interlocking and less porosity. The EDX spectrum for the stabilized material (Figure 22(c)) mostly displays O, Si, Al, and Ca, together with compositional characteristics indicative of the ceramic addition, including visible Mo, so corroborating the existence of aluminosilicate- and Ca-bearing phases. Collectively, these data indicate that the CW facilitates the precipitation of tiny binding gels (e.g., C–S–H/calcium-aluminosilicate hydrate (C–A–S–H)-type products), which enhance microstructural density and reinforce interparticle connections. This microstructural refinement offers a mechanistic rationale for the anticipated improvements in stiffness and compressive strength of the treated soil compared to the untreated control.

A clear loosening of interparticle links is observed following immersion. The unsoaked stabilized soil (Figure 22) has a thick microstructure, characterized by well-formed cementitious gels that connect the particles, creating a continuous bonding network. Following immersion (Figure 23), while the overall structure seems more compact and the pores are less discernible, the interparticle linkages exhibit reduced rigidity and softness due to water penetration and partial hydration of the binding phases. This technique diminishes the adhesive strength of the gel bridges and compromises their continuity, resulting in a more pliable particle structure. The EDX spectrum indicates a minor decrease in calcium intensity relative to the unsoaked condition, implying partial leaching or alteration of Ca-containing phases such C–S–H. This chemical alteration corroborates the microstructural evidence of bond relaxation, suggesting that soaking facilitates densification via rearrangement while concurrently diminishing the strength and stiffness of interparticle connections within the stable matrix.

Augmenting the CW content from 6% (Figure 22) to 8% (Figure 24) results in a distinct densification and fortification of the soil matrix. The SEM micrographs of the 6% sample exhibit a moderately compressed structure in which particles are interconnected by discontinuous cementitious gels, resulting in small residual voids. Conversely, the 8% stabilized soil demonstrates a more homogeneous and cohesive structure, marked by thicker gel coats and enhanced interparticle connections that nearly conceal the original grain boundaries. This suggests that the supplementary ceramic material improves pozzolanic interactions among silica, alumina, and calcium, resulting in increased production of binding products such C–S–H and C–A–S–H phases.

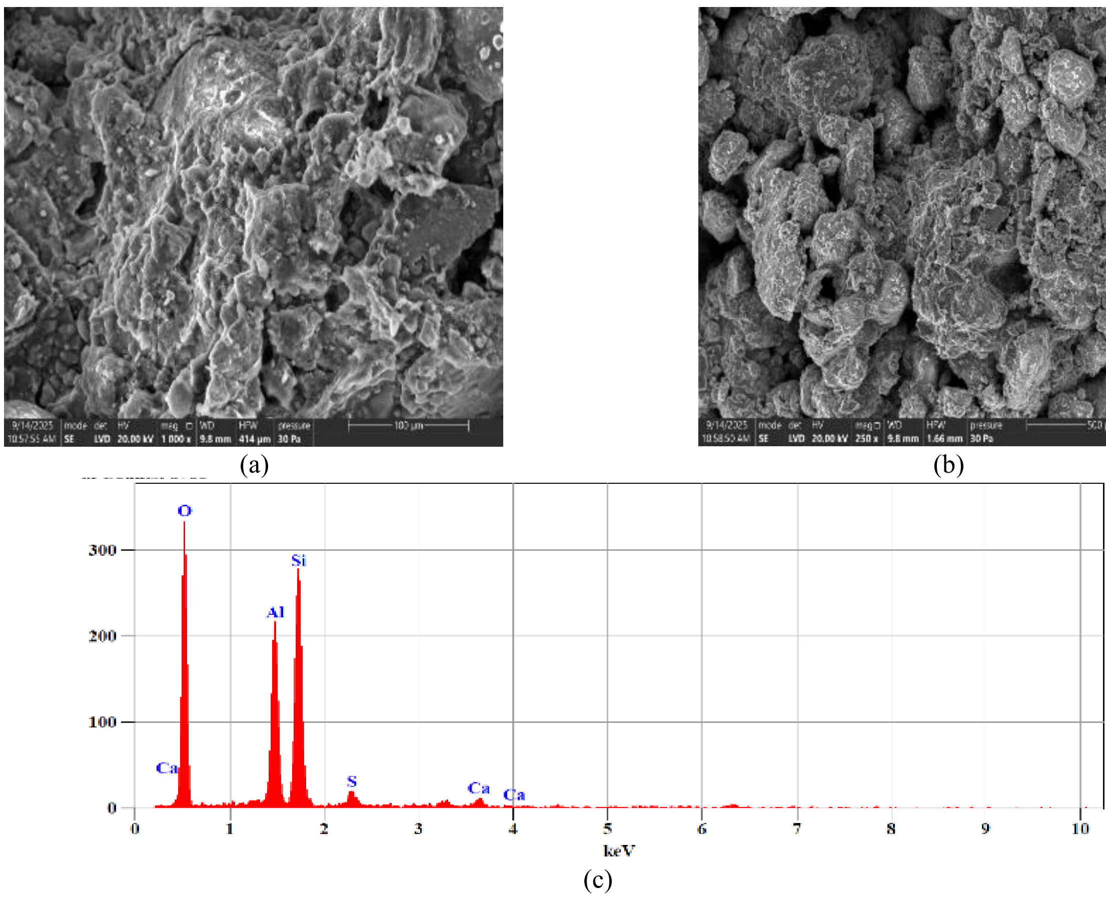

Figure 21. Microstructural and elemental characterization of the untreated soil (unsoaked; w = 6%; Ec = 60 blows): (a–b) SEM micrographs and (c) EDX spectrum

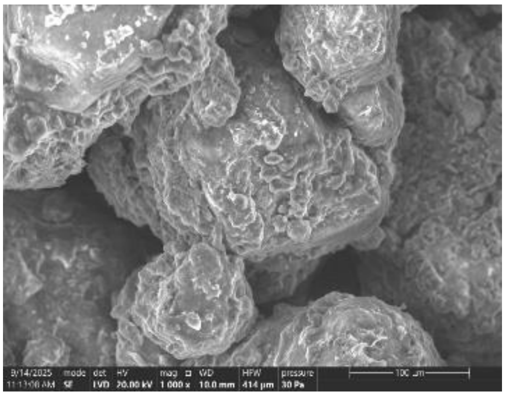

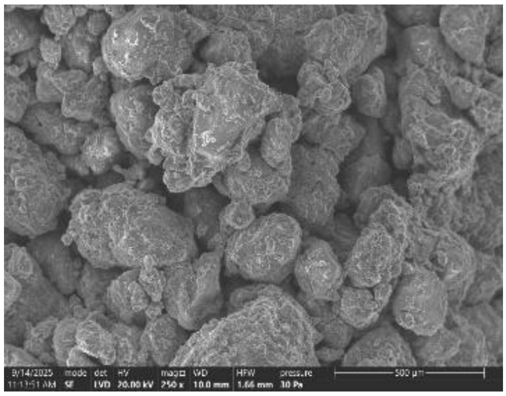

(a) (b)

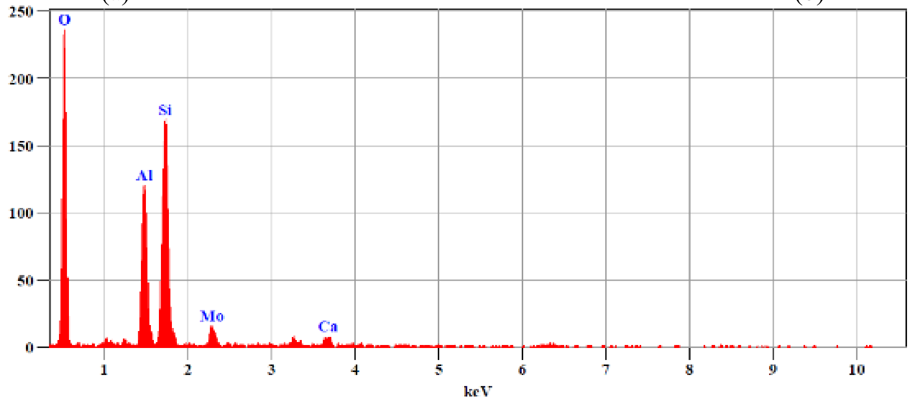

(c)

Figure 22. Microstructural and elemental characterization of the stabilized soil (unsoaked; 6% CW; w = 6%; Ec = 60 blows): (a–b) SEM micrographs and (c) EDX spectrum

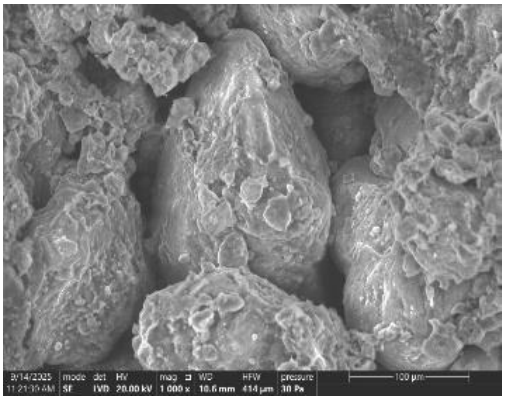

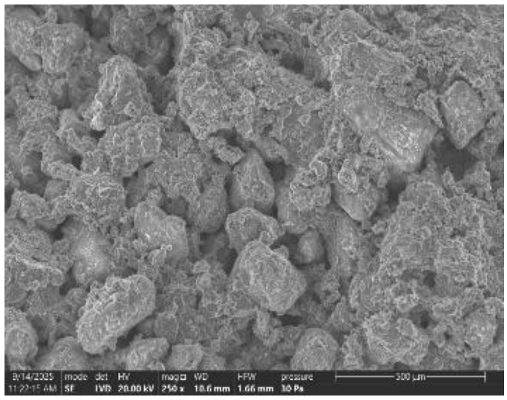

(a) (b)

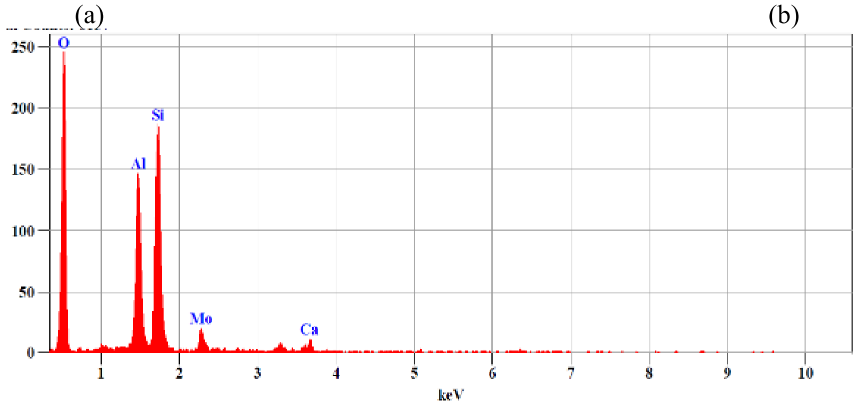

(c)

Figure 23. Microstructural and elemental characterization of the stabilized soil (soaked; 6% CW; w = 6%; Ec = 60 blows): (a–b) SEM micrographs and (c) EDX spectrum

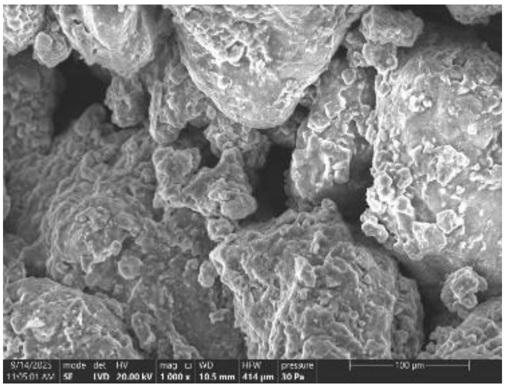

(a)

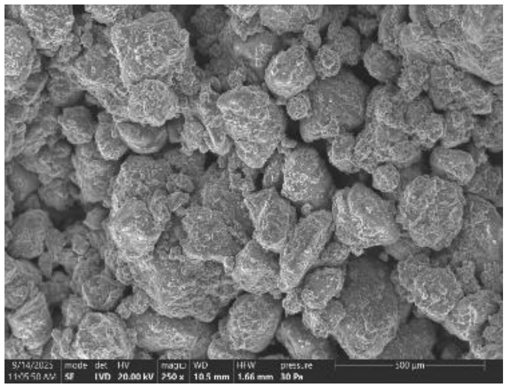

(b)

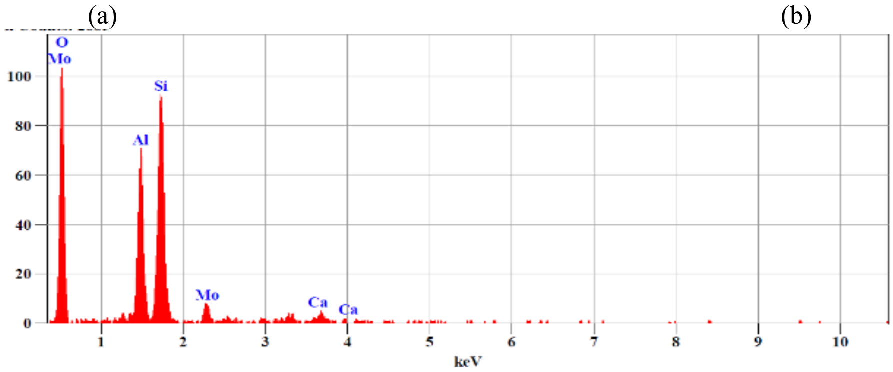

(c)

Figure 24. Microstructural and elemental characterization of the stabilized soil (unsoaked; 8% CW; w = 6%; Ec = 60 blows): (a–b) SEM micrographs and (c) EDX spectrum

The EDX spectra corroborate these findings: both samples exhibit the same predominant elements (O, Si, Al, Ca, Mo), but the 8% combination demonstrates comparatively elevated intensities of oxygen and silicon, indicating enhanced silicate phase development and increased gel integrity. The elevated ceramic content enhances microstructural densification, strengthens particle bonding, and decreases porosity, thus indicating an enhancement in mechanical strength and durability in unsaturated circumstances.

4. CONCLUSION

This research illustrates that finely milled CW serves as an efficient and sustainable stabilizer for collapsible soils prevalent in arid and semi-arid areas. The trials, utilizing locally sourced Algerian materials (Boussaâda sand, Djebel Debbagh kaolin, and CW from Aïn Azel), demonstrated substantial enhancements in both mechanical and microstructural properties. The plasticity index diminished from 8.66% (untreated) to 4.24% at 8% CW, however the maximum dry density augmented from 1.91 g/cm³ to 1.96 g/cm³ at 6% CW. With w = 6% and Ec = 60 blows, the collapse potential decreased from around 11.72% to less than 1%, categorizing the soil as non-collapsible. UU triaxial testing demonstrated a significant increase in cohesiveness from 16 to 105 kPa, accompanied by a little reduction in the friction angle (about 35.5° to 29.9°). SEM/EDX examinations verified the development of compact microstructures and refined cementitious gels (C–S–H/C–A–S–H) interconnecting soil particles. The microstructural alterations elucidate the observed improvement in strength and durability. Recycling CW offers a cost-effective and environmentally efficient approach to soil stability while fostering sustainable waste management and ground enhancement practices in Algeria and other dry areas.

REFERENCES

[1] Derbyshire, E., Dijkstra, T.A., Smalley, I.J., Li, Y. (1994). Failure mechanisms in loess and the effects of moisture content changes on remoulded strength. Quaternary International, 24: 5-15. https://doi.org/10.1016/1040-6182(94)90032-9

[2] Marković, S., O'Hara-Dhand, K., McLaren, S. (2015). Ian Smalley: The genius of loess of the loess world. Quaternary International, 372: 1-5. https://doi.org/10.1016/j.quaint.2015.05.028

[3] Li, Y., Shi, W., Aydin, A., Beroya-Eitner, M.A., Gao, G. (2020). Loess genesis and worldwide distribution. Earth-Science Reviews, 201: 102947. https://doi.org/10.1016/j.earscirev.2019.102947

[4] Rogers, C.D.F. (1995). Types and distribution of collapsible soils. In Genesis and Properties of Collapsible Soils, pp. 1-17. https://doi.org/10.1007/978-94-011-0097-7_1

[5] Nouaouria, M.S., Guenfoud, M., Lafifi, B. (2008). Engineering properties of loess in Algeria. Engineering Geology, 99(1-2): 85-90. https://doi.org/10.1016/j.enggeo.2008.01.013

[6] Gaaver, K.E. (2012). Geotechnical properties of Egyptian collapsible soils. Alexandria Engineering Journal, 51(3): 205-210. https://doi.org/10.1016/j.aej.2012.05.002

[7] Ouatiki, K., Bahi, L., Awa, M.O., Ouadif, L., Akhssas, A., Ejjaaouani, E.H. (2016). Identification of collapsible soils in Deroua (Morocco). European Scientific Journal, ESJ, 12(6): 255. https://doi.org/10.19044/esj.2016.v12n6p255

[8] Houston, S.L., Houston, W.N., Spadola, D.J. (1988). Prediction of field collapse of soils due to wetting. Journal of Geotechnical Engineering, 114(1): 40-58. https://doi.org/10.1061/(ASCE)0733-9410(1988)114:1(40)
[9] Clemence, S.P., Finbarr, A.O. (1981). Design considerations for collapsible soils. Journal of the Geotechnical Engineering Division, 107(3): 305-317. https://doi.org/10.1061/AJGEB6.0001102
[10] Opukumo, A.W., Davie, C.T., Glendinning, S., Oborie, E. (2022). A review of the identification methods and types of collapsible soils. Journal of Engineering and Applied Science, 69: 17. https://doi.org/10.1186/s44147-021-00064-2
[11] Jennings, J.E., Knight, K. (1957). The additional settlement of foundations due to a collapse of structure of sandy subsoils on wetting. In 4th International Conference on Soil Mechanics and Foundation Engineering, London, pp. 316-319.
[12] El Howayek, A., Huang, P.T., Bisnett, R., Santagata, M.C. (2011). Identification and behavior of collapsible soils. Purdue University. https://doi.org/10.5703/1288284314625
[13] ASTM (2026). ASTM D4546 – Standard Test Methods for One-Dimensional Swell or Collapse of Soils.
[14] Zanin, R.F.B., Kondo, A.M., Pelaquim, F.G.P., et al. (2024). The impact of gradual increase in moisture on the collapse of Brazilian clayey sand soil. Bulletin of Engineering Geology and the Environment, 83: 36. https://doi.org/10.1007/s10064-023-03523-7
[15] Saftner, D., Dagger, R. (2018). Cone penetration testing manual for highway geotechnical engineers.
[16] Berisavljević, D., Rakić, D., Šušić, N. (2015). SDMT–A tool for in situ identification of collapsible soils. In Proceedings of the 3rd International Conference on the Flat Dilatometer DMT, pp. 457-463.
[17] Cui, Y.J., Delage, P. (1996). Yielding and plastic behaviour of an unsaturated compacted silt. Géotechnique, 46(2): 291-311. https://doi.org/10.1680/geot.1996.46.2.291
[18] Delage, P., Audiguier, M., Cui, Y.J., Howat, M.D. (1996). Microstructure of a compacted silt. Canadian Geotechnical Journal, 33(1): 150-158. https://doi.org/10.1139/t96-030
[19] Lawton, E.C., Fragaszy, R.J., Hardcastle, J.H. (1989). Collapse of compacted clayey sand. Journal of Geotechnical Engineering, 115(9): 1252-1267. https://doi.org/10.1061/(ASCE)0733-9410(1989)115:9(1252)
[20] Ménard, L., Broise, Y. (1975). Theoretical and practical aspect of dynamic consolidation. Geotechnique, 25(1): 3-18. https://doi.org/10.1680/geot.1975.25.1.3
[21] Rollins, K.M., Kim, J. (2010). Dynamic compaction of collapsible soils based on U.S. case histories. Journal of Geotechnical and Geoenvironmental Engineering, 136(9): 1178-1186. https://doi.org/10.1061/(ASCE)GT.1943-5606.0000331
[22] Bell, F. (1996). Lime stabilization of clay minerals and soils. Engineering Geology, 42(4): 223-237. https://doi.org/10.1016/0013-7952(96)00028-2
[23] Consoli, N.C., Lopes Jr, L.D.S., Prietto, P.D.M., Festugato, L., Cruz, R.C. (2011). Variables controlling stiffness and strength of lime-stabilized soils. Journal of Geotechnical and Geoenvironmental Engineering, 137(6): 628-632. https://doi.org/10.1061/(ASCE)GT.1943-5606.0000470
[24] Ayeldeen, M., Azzam, W., Arab, M.G. (2022). The use of fiber to improve the characteristics of collapsible soil stabilized with cement. Geotechnical and Geological Engineering, 40: 1873-1885. https://doi.org/10.1007/s10706-021-01997-4
[25] Bahloul, O., Abbeche, K., Bahloul, A. (2016). Study of the microstructure of collapsible soil treated with the potassium chloride. Journal of Applied Engineering Science and Technology, 2(1): 4. https://doi.org/10.69717/jaest.v2.i1.30
[26] Bakir, N., Abbeche, K., Panczer, G. (2017). Experimental study of the effect of the glass fibers on reducing collapse of a collapsible soil. Geomechanics and Engineering, 12(1): 71-83. https://doi.org/10.12989/gae.2017.12.1.071
[27] Habib, M.S., El Sawwaf, M.A., Shahien, M.M., Nasr, A.M. (2025). Using biopolymers to stabilize collapsible soil by using wet mix method. Indian Geotechnical Journal, 55(5): 2738-2750. https://doi.org/10.1007/s40098-024-01075-5
[28] Soldo, A., Miletić, M., Auad, M.L. (2020). Biopolymers as a sustainable solution for the enhancement of soil mechanical properties. Scientific Reports, 10(1): 267. https://doi.org/10.1038/s41598-019-57135-x
[29] Abaas, R.F., Fattah, M.Y., Naif, M.H., Hafez, M. (2024). Collapsible gypseous soil stabilization by calcium carbide residue and sulfonic acid. Sustainability, 16(22): 9974. https://doi.org/10.3390/su16229974
[30] Lavat, A.E., Trezza, M.A., Poggi, M. (2009). Characterization of ceramic roof tile wastes as pozzolanic admixture. Waste Management, 29(5): 1666-1674. https://doi.org/10.1016/j.wasman.2008.10.019
[31] Attaelmanan, M., Kambal, M.E.M., Mansour,M.I. (2021). A study the effect of using ceramic waste powder as partial replacement for cement on concrete properties. Journal of Karary University for Engineering and Science, 1(1). https://doi.org/10.54388/jkues.v1i1.125
[32] Hoppe Filho, J., Pires, C.A.D.O., Leite, O.D., Garcez, M. R., Medeiros, M.H.F.D. (2021). Red ceramic waste as supplementary cementitious material: Microstructure and mechanical properties. Construction and Building Materials, 296: 123653. https://doi.org/10.1016/j.conbuildmat.2021.123653
[33] Matias, G., Faria, P., Torres, I. (2014). Lime mortars with ceramic wastes: Characterization of components and their influence on the mechanical behaviour. Construction and Building Materials, 73: 523-534. https://doi.org/10.1016/j.conbuildmat.2014.09.108
[34] Rathore, P., Tiwari, S.K. (2023). Soil stabilization using ceramic waste: An experimental study. Journal of Mining and Environment, 14(1): 47-65. https://doi.org/10.22044/jme.2023.12442.2259
[35] Iravanian, A., Saber, S.A. (2020). Using ceramic wastes in stabilization and improving soil structures: A review study. IOP Conference Series: Earth and Environmental Science, 614(1): 012081. https://doi.org/10.1088/1755-1315/614/1/012081
[36] Blayi, R.A., Omer, B., Ababakr, F.A., Yaseen, B.S., Jober, A.M., Hisqel, A.S. (2026). Impact of ceramic waste powder on the geotechnical properties of a clayey soil. Next Materials, 11: 101863. https://doi.org/10.1016/j.nxmate.2026.101863

[37] Saber, S.A., Iravanian, A. (2022). Using waste ceramic dust in stabilization of clay soils. International Journal of Sustainable Construction Engineering and Technology, 13(1): 68-80. https://doi.org/10.30880/ijscet.2022.13.01.007

[38] Okeke, C.A. (2020). Engineering behaviour of lime-and waste ceramic dust-stabilized expansive soil under continuous leaching. Bulletin of Engineering Geology & the Environment, 79(4): 2169-2185. https://doi.org/10.1007/s10064-019-01648-2

[39] ASTM. (2017). ASTM D4318 – Standard Test Methods for Liquid Limit, Plastic Limit, and Plasticity Index of Soils. ASTM International.

[40] ASTM. (2017). ASTM D5333 – Standard Test Method for Measurement of Collapse Potential of Soils. ASTM International.

[41] ASTM. (2021). ASTM D698 – Standard Test Methods for Laboratory Compaction Characteristics of Soil Using Standard Effort (12,400 ft-lbf/ft3 (600 kN-m/m3)). ASTM International.

[42] ASTM. (2026). ASTM D2850 – Standard Test Method for Unconsolidated-Undrained Triaxial Compression Test on Cohesive Soils. ASTM International.

[43] Chen, J.A., Idusuyi, F.O. (2015). Effect of waste ceramic dust (WCD) on index and engineering properties of shrink-swell soils. International Journal of Engineering and Modern Technology, 1(8): 52-62.

[44] Sabat, A.K., Pati, S. (2014). A review of literature on stabilization of expansive soil using solid wastes. Electronic Journal of Geotechnical Engineering, 19(6): 6251-6267.

NOMENCLATURE

CW	Ceramic waste
CP	Collapse potential
γdma	maximum dry density
wopt	optimum moisture content
τ	shear strength
σ	normal strength
c	cohesion
φ	internal friction angle
UU	unconsolidated undrained
Ec	Compaction Energy
w	water content